New Results of Research into Mixture Formation in the Direct Injection Diesel Engine

K.Binder and V.Pfeffer

Daimler-Benz AG
Abteilung FVA/V
Postfach 600 202
7000 Stuttgart 60
F.R.Germany

Abstract

Increasing injection pressure makes mixture formation less dependent on air swirl. Particularly in the lower engine speed range where swirl is always low and the duration of injection short, this offers benefits in terms of fuel consumption and black smoke emission. As the improved mixture formation allows the engine to be operated with a considerably retarded start of injection, there is no detrimental effect on nitrogen oxide emissions despite more rapid combustion.

Studies have revealed that the decisive mechanism is the interaction of the fuel drops in the jet. However, this interaction is determined less by maximum injection pressure than by the injection pressure history. A constant rise in pressure up to maximum injection pressure is desirable. As the interaction cannot be effective during the entire phase of the pressure drop (closing phase), experience has shown that this phase should be designed to be very short.

Increasing the number of injector holes results in an additional boost being given to this in-jet interaction which promotes mixture formation.

1. Introduction

Although commercial vehicle direct-injection diesel engines have undergone enormous development in the last 25 years and, as revealed by Figure 1, on the basis of the specific power output and the power to weight ratio, have attained a high development standard (1). The Research & Development Departments of engine manufacturers have been devoting enormous resources to improving internal engines processes in order to satisfy the often contradictory objectives, demands and wishes in respect, for example, of emissions, noise, fuel consumption or comfort. This is achieved, on the one hand, by specifically varying and combining possible influencing variables, on the other hand, though, by analysing the mixture formation and combustion of the parameters involved. The latter method has formed the basis of the knowledge and correlations presented in this paper.

In view of the fact that it is by no means a straight-forward matter in real-life engine operation to separate and quantify individual influencing parameters, the problem has to be tackled by applying experimental and measuring techniques and, where possible, also, by drawing on physical mathematical models for analysis.

For this reason, the correlations described below were investigated by examining not only single-cylinder test engines, but also combustion bombs and computer modelling methods. The procedure selected is illustrated in greater detail on the basis of the injection pressure.

2. Procedure

Quantifying the sole influence of injection pressure on the principal engine characteristics of consumption and emissions over the entire engine performance map necessitates eliminating other influencing factors such as engine speed and thus squish or swirl but also injection pressure or duration of injection, or, by adapting an appropriate procedure, incorporating them in the assessment.

As the duration of injection in degrees crank angle is prolonged with engine speed, for example, where the quantity injected is fixed, while swirl remains practically constant with engine speed, optimal air utilization can thus only exist in one point of the map (refer to Figure 2). At engine speed n_2, the duration of injection ID_0 is just as long as to further rotate the column of air rotating around the piston bowl axis at the swirl determined by inlet port design and just prevent drifting occurring, as is the case at n_2 and the related angle β_2. At engine speed n_1 the duration of in-

jection is too short or the swirl too low, with the result that the air is rotated only to β_1. Both cases result in local over-enriching and the quantitiy of fuel injected being reduced. The consequence is an unsatisfactory bmep versus engine speed.

The problem is thus to optimally match duration of injection and swirl over the entire engine performance map. As squish and, particularly, injection pressure also increase with engine speed, it is not a straight-forward matter to properly quantify the individual influences acting on mixture formation and combustion, and thus on engine characteristics. It is possible to get round this problem by operating at a constant engine speed, maintaining the quantitiy injected and thus also the duration of injection at a constant level, and steplessly varying swirl. As shown in Figure 2, the low swirl level then corresponds to the lower engine speeds and the high swirl level to the high engine speeds.

3. Determining Engine Characteristics

3.1 Test Medium

3.1.1 Test Engine

To achieve symmetrical conditions in respect of squish flow, a single-cylinder engine with 4 valves per cylinder (1 inlet port covered on one side, effected as an directed port, 1 inlet port with shrouded valve) was selected as the test engine. The principal data is listed in Figure 3.

The inlet port was provided with a shrouded valve which can be pivoted when the engine is running, in order to steplessly alter the swirl. The arrangement of the ports and valves vis-a-vis the cylinder is shown schematically in Figure 4, top. The attainable swirl is plotted as a function of the position of the shrouded valve in Figure 4, bottom.

To examine the question of whether the swirl attainable in this way with the shrouded valve can be quated in terms of mixture formation and flame propagation with the swirl produced in the usual way in automotive engineering by means of helical inlet ports, helical inlet ports with swirl stages D_1 (standard) and D_2 as well as with swirl D_3 were represented and compared with the swirl stages of shroud positions α = 0°, -75°, -120° and -150° by using a high speed camera. The film engine used for this comparison is shown in Figure 5. With the exception of case D_3, jet and flame propagation behave practically identically. Engine characteristics were also found to be within a narrow scattering range. The very low swirl level D_3 needs a shroud position, which produce an extreme counter swirl to the drected port. This results in severe shear flows and turbulences. In comparison to the inlet ports combustion therefore progresses at a much faster rate. The very low swirl level D_3 was therefore regarded carefully during the remaining test procedure.

3.1.2 Injection System

The hydraulically actuated unit injector developed by Bosch and shown schematically in Figure 6, was adapted to the test engine in order to represent the different injection pressures at a constant injection duration. It is possible to harmonize peak pressure and duration of injection over wide limits by selecting system pressure, working plunger, pump plunger and injector hole diameter. All the influencing parameters were appropriately collated in a catalogue, enabling the setup to be selected which produces the same injection durations for different peak pressures or as shown in Figure 7, different durations of injection for the same peak pressures. Particular care was paid to selecting setups which, as far as possible, produced identical opening and closing edges.

3.2 Test Procedure

Maximum injection pressures of 600 bar, 1200 bar and 1800 bar were represented for an injected quantitiy of approximately 100 mm^3/cycle and a duration of injection of 20° CA at n = 1800 rpm, and, the effects on black smoke, nitrogen oxide and CO emissions were examined. The start of injection was varied in small steps to check the plausibility of the results. The earliest start of injection was 20° CA bTDC (injection at TDC just completed), the latest at 10° CA bTDC (symmetrical injection to TDC). With the engine running, swirl was increased in stages from 0.2 to 2.6. The majority of tests were conducted with 4-hole nozzles, although 8-hole nozzles were also used in spot tests to check the working hypothesis. The piston bowl was a constant 88 mm diameter. Compression ratio was 16 : 1.

3.3 Test Results

Black smoke and specific fuel consumption are presented in Figure 8 as a function of swirl. The parameters being maximum injection pressure and start of injection. The boundary lines of the range shown represent the results for earliest and latest start of injection. At a pressure of 1800 bar, the earliest start of injection was at 16° CA in view of the pressure rise and the maximum combustion pressure. As expected, black smoke and consumption improve as the start of injection is advanced, since the soot-producing diffusion flame diminishes as a result of enlarging the share of the premixed flame and the efficiency-promoting constant-volume share of combustion increases. The effect, however, diminishes as swirl increases and, notably, with in-

creasing injection pressure.

A striking feature is that, when duration of injection and swirl are optimally harmonized (this being the case for instance for swirl D = 2.6 at the selected duration of injection of 20 ° CA), it is practically impossible to determine any effect of maximum injection pressure on consumption and black smoke. At low swirl - corresponding, as already stated, to the lower rpm range in the engine map - the increase in injection pressure has an increasingly positive impact, however.

These correlations are shown also in Figure 9 in which the CO emissions are presented as a function of swirl as an indicator for quality of mixture formation.

Figure 10 shows first of all the known conflicting aims between smoke, consumption and CO on the one hand, and NO_x on the other hand. Maximum NO_x emissions being measured when duration of injection and swirl are optimally harmonized.

Increasing maximum injection pressure, though, enables the engine to be operated with a later start of injection, permitting clear benefits in respect of black smoke and CO to be achieved as a result of the lower swirl sensitivitiy in the lower swirl range without any concomitant drawbacks in terms of consumption and NO_x.

In view of the fact that the existing shrouded valve arrangement enables swirl to be increased only to D = 2.7, no rise of bsfc, SZ (black smoke) and NO_x was observed in the upper swirl range at the selected duration of injection. The very sharp increase of SZ as a result of drifting could be demonstrated, though, by extending the duration of injection or, as shown in Figure 11, 12 and 13, by switching from the 4-hole to the 8-hole nozzle (with no change injection duration). Drifting causes fuel consumption, black smoke and, above all, CO to rise sharply, and NO_x emissions to diminish.

4. Determining the Mechanism

After demonstrating that the effect of increasing injection pressure on engine behaviour depends greatly on harmonization of injection duration and swirl, the next step was to examine the mechanisms involved when injection pressure is increased, by conducting experiments outside of the engine.

4.1 Test Medium

Use was made of the film engine shown in Figure 5 to determine injection jet geometry, jet penetration depth, interaction of jet and combustion chamber wall, ignition point and of swirl.

The fuel jet was injected into a combustion bomb to determine droplet velocities by means of laser velocimetry, it being possible to vary not only the injection parameters of pressure and quantitiy but also the back-pressure and air movement in the bomb.

4.2 Test Results

As injection pressure rises, jet peak velocity - as expected - increases. Consequently, the jet injected also strikes the combustion chamber wall at a higher velocity, which affects the jet/ wall interaction.

With increasing injection pressure, the ignition point migrates away from the nozzle, to shift back again as swirl increases. Increasing injection pressure shortens the duration of combustion only if swirl and duration of injection are not optimally harmonized.

Surprisingly, jet geometry (jet cone angle, jet diameter) depends only slightly on injection pressure, even if the latter - as shown in Figure 14 - is boosted from 600 bar to 1800 bar. At least, it appears unlikely that the sharp differences in engine characteristics determined in the lower swirl range can be explained by jet geometry.

Figure 15 shows the axial droplet velocity versus time for a measuring point in the geometrical jet axis 50 mm away from the injector. The combustion bomb was filled with static nitrogen. The gas pressure in the chamber was 10 bar, temperature 300 K, maximum injection pressure 600 bar. The velocity of the droplets climbs initially from approximately 50 m/s to maximum levels of approximately 75 m/s, to then drop steadily again toward end of injection. A striking feature is that droplet velocities in the tail of the jet display practically no scatter. By contrast, severe scatter is present at the beginning of the jet and in the middle phase of injection. Similar results were found by varying the measuring point (edge of jet) and at a greater distance from the nozzle, and by varying the gas pressure in the chamber and the injection pressure.

If we look at the theoretically determined jet penetration depth presented in Figure 16 as a function of time and take the effective injection pressure history presented in Figure 17 as the basis, it is clearly revealed that the fuel injected at a lower pressure at the commencement of injection is very rapidly "overtaken" by the fuel which is injected later but at a higher pressure.

This "overtaking" results in interaction of the individual fuel drops or segments in the jet, which in turn produce small droplets with differing velocities. This

applies in principle until maximum injection pressure is reached. Similar results were obtained also in (2).

This mixture formation-promoting interaction no longer takes place once maximum injection pressure is reached, as the fuel injected subsequently now has a lower initial velocity. Experience has shown, that therefore a slow drop of the injection process must be avoided. The physical reason was found in the lack of interaction in the jet in this case.

It, therefore, also becomes clear that the critical factor is not the maximum injection pressure, which anyway prevails only for an extremely short period, but the pressure gradient.

To exemplify this, raising the nozzle opening pressure does promote the jet pulse and thus the penetration depth, but not the interaction in the injection jet. How important this pulse interaction in the jet is in terms of good mixture formation is illustrated by Figure 11 to 13, which have already been discussed. The 8-hole nozzle presented here displays even less swirl dependence than the 4-hole nozzle operated at 1800 bar peak pressure. There are essentially three reasons for this:

- Increasing the number of injection jets enhances the possibility of pulse interaction in the jet
- As injection pressure rises, the wall portion does rise, but less than with the 4-hole injector in view of the lower jet pulse
- An extremely high maximum injection pressure generally extends the unfavourable closing phase.

Attention also requires to be given to increasing the number of injection holes, though, as the jet pulse is reduced if the injection equipment otherwise remains constant. Particularly with turbocharging, this can result in the air not being sufficiently utilized.

4.3 Computer Modelling

Jet peak velocity, drop size distribution and drop velocity were determined for two extreme injection rates (Figure 18) to assist the mechanisms determined. Figure 19 shows drop velocity for injection rate 1 and a single-hole nozzle at a distance of 20.5 mm from the injector. Drop velocities give absolutely no indication of interaction within the jet. As the jet pulse drops when a switch is made from 1-hole to 4-hole nozzles, drop velocity - as shown in Figure 20 - decreases. Interaction occurs in isolated cases, with the result that the velocity range increases.

The pulse of the 8-hole nozzle shown in Figure 21 is again lower. The fuel droplets increasingly collide, producing a further rise in the velocity scatter. A look at injection rate 2 reveals that the pressure rises continuously from start of injection to practically end of injection. The pressure gradient of the 1-hole nozzle (Figure 22) is still too steep, resulting only in slight interaction. This occurs more so with the 4-hole nozzle (Figure 23) and to an even more pronounced extent with the 8-hole nozzle (Figure 24). A comparison of Figures 21 and 24 reveals, that in the case of injection rate 1 the maximum droplet velocity is smaller and the scatter greater than in the case of injection rate 2. Interaction in the case of injection pattern 2, however, continues practically until the end of injection. The effect of interaction in the injection jet on mean droplet velocity and thus on jet decay can therefore be assisted by modelling.

5. References

(1) Mischke, Klünder

Die Entwicklung der Mechanik der neuen Mercedes-Benz Nutzfahrzeug-Motoren
MTZ 02/86

(2) Winklhofer

Abschlußbericht FVV-Vorhaben Nr. 355
Strahlenausbreitung
Forschungsberichte Verbrennungskraftmaschinen
Heft Nr. 426/1988

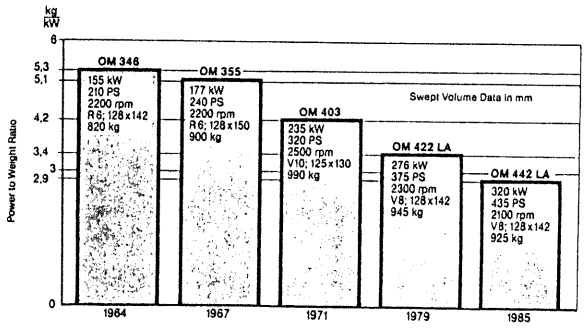

Figure 1

Reduction of the Power to Weight Ratio of True Engines

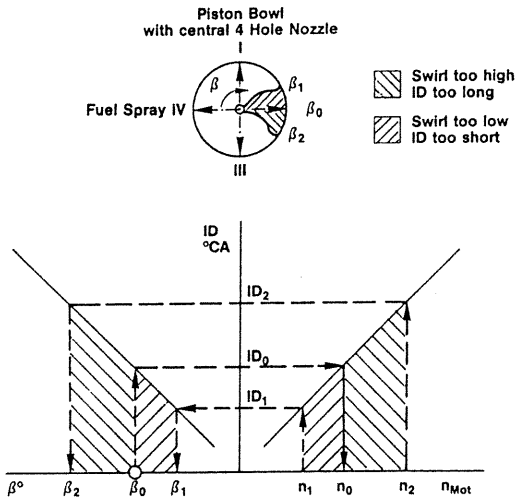

Figure 2

Injection Duration ID and Swirl versus Engine Speed

Bore	**Ø 128 mm**
Stroke	**Ø 150 mm**
Piston Bowl Diameter	**Ø 88 mm**
Compression Ratio	**16 : 1**

4 Valves

Helical Port / Directed Port with Shrouded Valve

Variable Swirl

Hydraulically actuated Unit / Injector

Nozzle 4 × Ø 0,30 mm Injection Pressure 600 bar

Nozzle 4 × Ø 0,26 mm Injection Pressure 1200 bar

Nozzle 4 × Ø 0,21 mm Injection Pressure 1800 bar

Engine Speed 1800 rpm

Figure 3

Engine Data of the Single Cylinder Test Engine

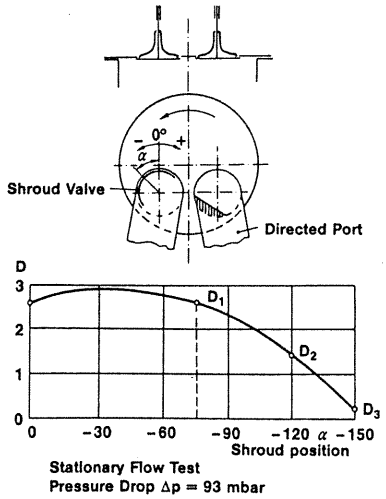

Figure 4

Swirl D versus Shroud Position

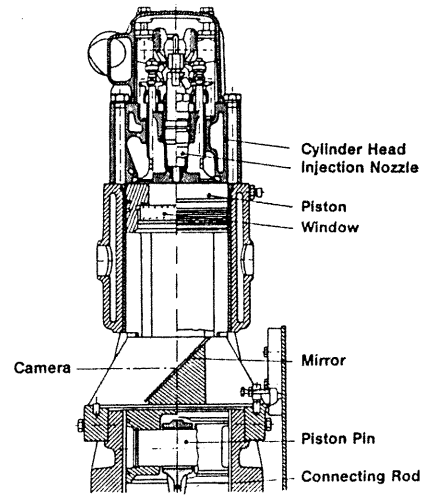

Figure 5

Setup of the Film Engine

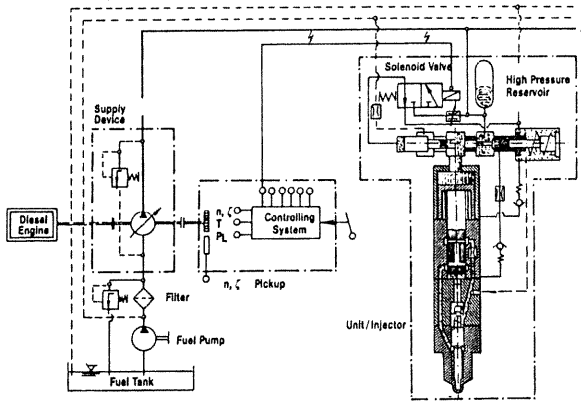

Figure 6

Setup of the Hydraulically Actuated Unit Injector

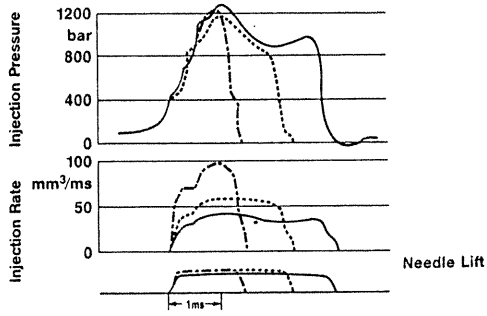

			Design and Tuning of Injection System			
	ID ms	P_{Emax} bar	d mm	P_{sys} bar	d_{AK} mm	d_{pk} mm
———	3.7	1200	0.19	100	20	6
– – –	2.7		0.23	110	20	6
–·–·–	1.7		0.29	132	20	6

Figure 7

Variation of the Injection Duration at constant Peak Injection Pressure

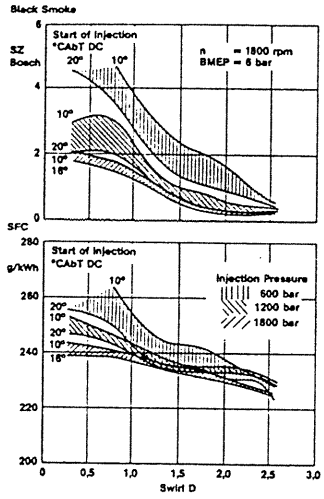

Figure 8

Influence of the Injection on Black Smoke SZ and Specific Fuel Consumption SFC
4-Hole-Nozzle, ID = 20 °CA

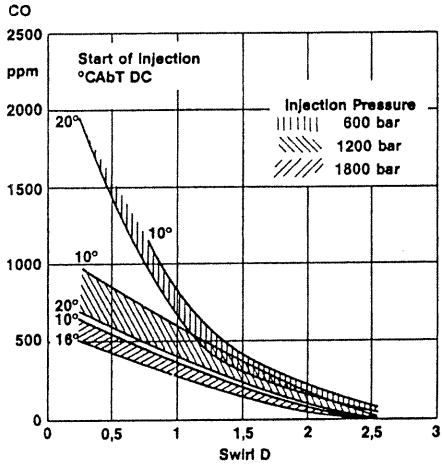

Figure 9

Influence of the Injection Pressure on the CO-Emission.
4-Hole-Nozzle, n = 1800 rpm, BMEP = 6 bar, ID = 20 °CA

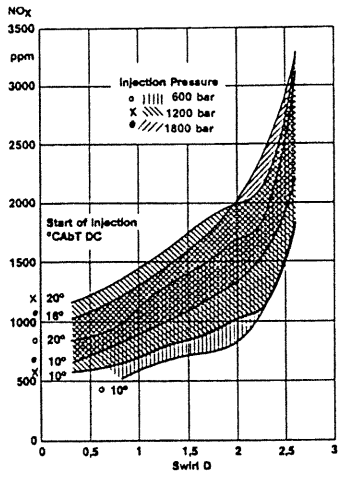

Figure 10

Influence of the Injection pressure on the NO_X-Emission.
4-Hole-Nozzle, n = 1800 rpm, BMEP = 6 bar, ID = 20 °CA

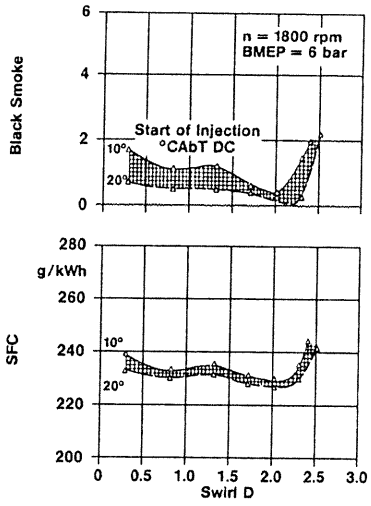

Figure 11

Influence of the Swirl D on Black Smoke and Specific Fuel Consumption SFC.
8-Hole-Nozzle, Peak Injection Pressure 600 bar, ID = 20 °CA

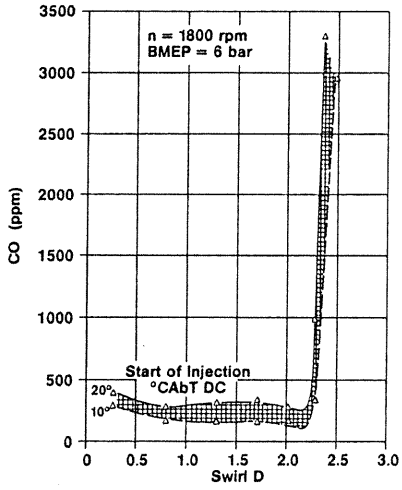

Figure 12

Influence of the Swirl on the CO-Emission.
8-Hole-Nozzle, Peak Injection Pressure 600 bar, ID = 20 °CA

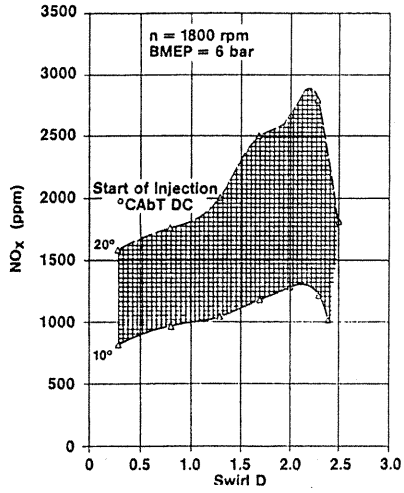

Figure 13

Influence of the Swirl D on the NO_X-Emission.
8-Hole-Nozzle, Peak Injection Pressure 600 bar, ID = 20 °CA

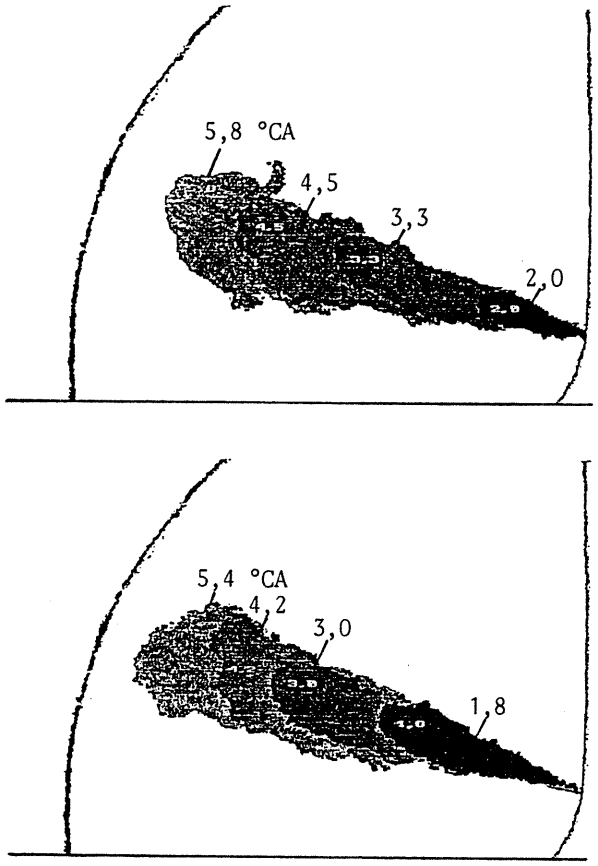

Figure 14

Geometrie of the Jet at Injection pressure of 600 bar and 1800 bar at Different Timing

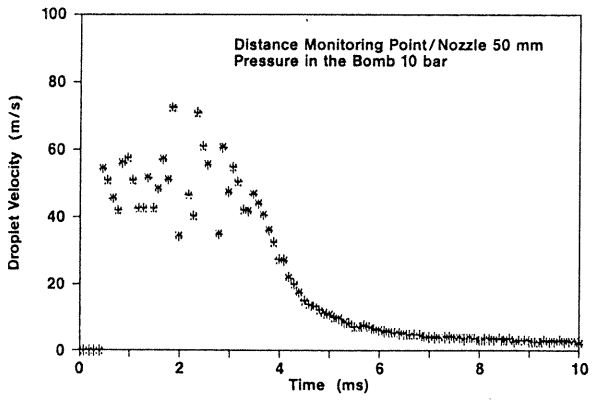

Figure 15

Measured Axial Jet Velocity versus Time. Medium in the Bomb: Nitrogen

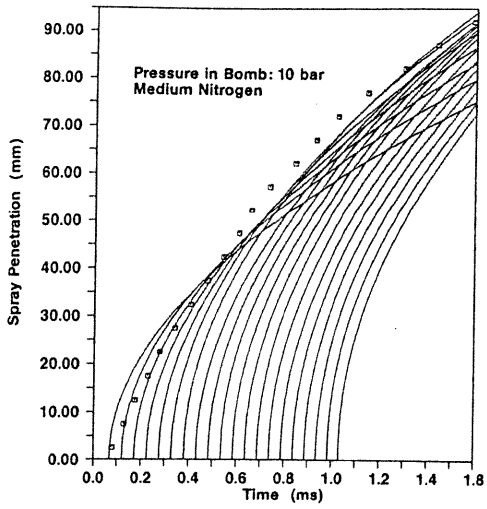

Figure 16

Computed Penetration Depth of the Jet at Different Timing

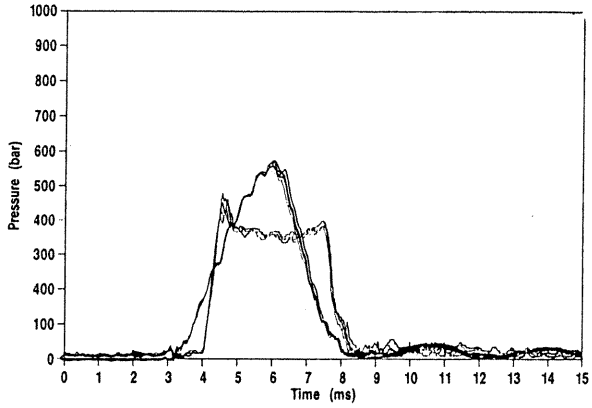

Figure 17

Needle Lift and Injection Pressure versus Injection Time

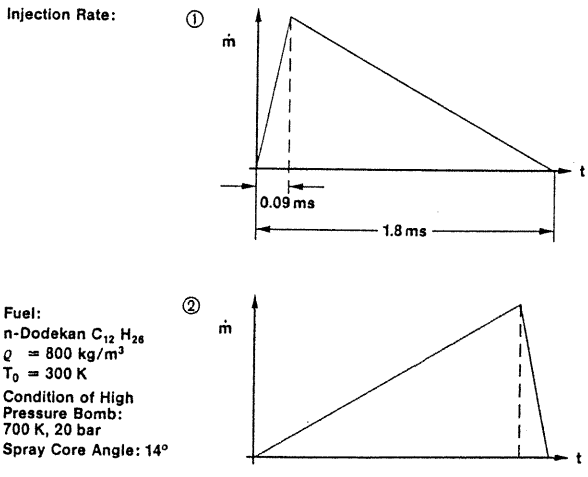

Figure 18

Injection Rates for Computation of the Droplet Velocity

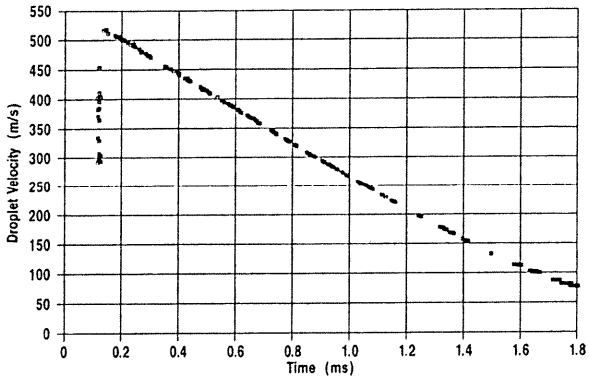

Figure 19

Computed Droplet Velocity.
1-Hole-Nozzle, Injection Rate 1,
Distance from the Nozzle 20,5 mm

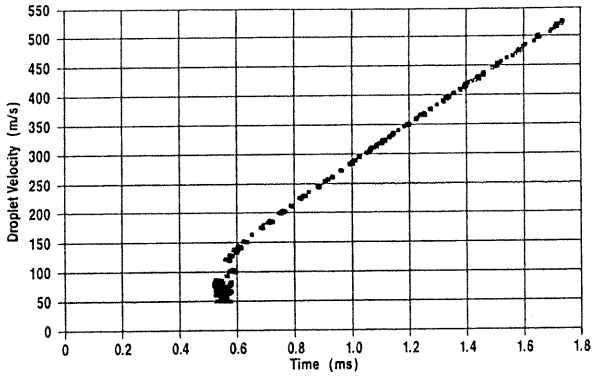

Figure 22

Computed Droplet Velocity.
1-Hole-Nozzle, Injection Rate 2,
Distance from the Nozzle 20,5 mm

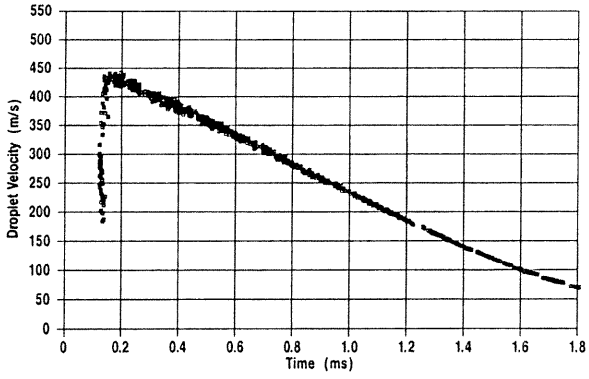

Figure 20

Computed Droplet Velocity.
4-Hole-Nozzle, Injection Rate 1,
Distance from the Nozzle 20,5 mm

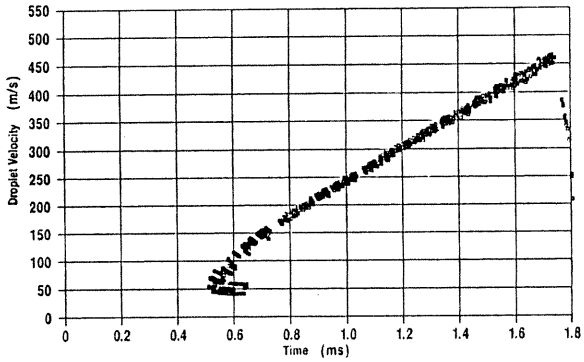

Figure 23

Computed Droplet Velocity.
4-Hole-Nozzle, Injection Rate 2,
Distance from the Nozzle 20,5 mm

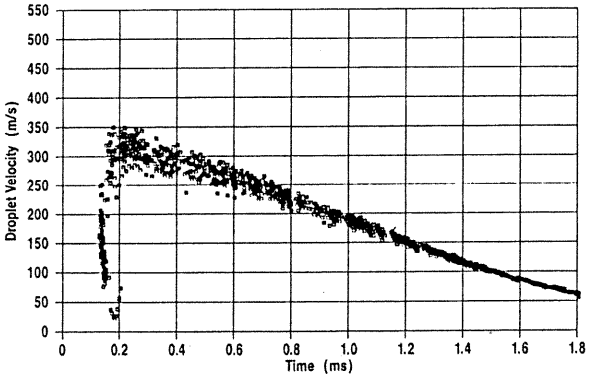

Figure 21

Computed Droplet Velocity.
8-Hole-Nozzle, Injection Rate 1,
Distance from the Nozzle 20,5 mm

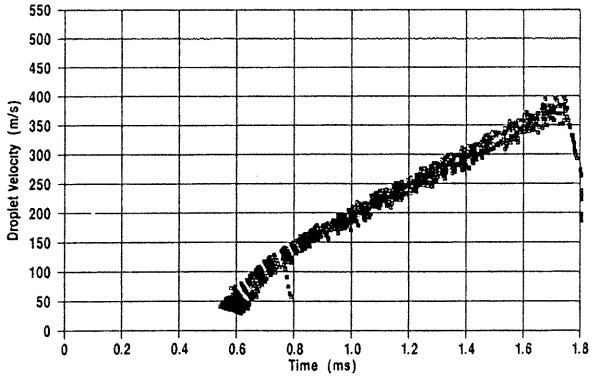

Figure 24

Computed Droplet Velocity.
8-Hole-Nozzle, Injection Rate 2,
Distance from the Nozzle 20,5 mm